

Comparative Radiation Dose Study of a Hypothetical Accident in a Research Reactor

A. Dahia,* D. Merrouche, A. Dadda, and A. L. Cheridi

Nuclear Research Center of Birine, B.P 180 Ain Oussera, Djelfa, 17 200, Algeria

This work is licensed under a
Creative Commons Attribution 4.0
International License



Abstract

This study is a contribution for radiation dose calculations of a hypothetical accident of a 1 MW research reactor Triga Mark II using HotSpot code. A postulated accidental release of noble gases and halogens were considered. The total effective dose (TED) was estimated for 1 day and 50 years after release. The total damage of fuel element cladding with a maximum radioactivity was considered. The obtained results show minimal TED values at the beginning of the release and at a shorter distance from the source. The maximum calculation results are acceptable and below the recommended public dose limit.

Keywords

Annual effective dose, atmospheric dispersion, TED, CEDE, HotSpot code, safety analysis

1 Introduction

The simulation of radioactive materials releases following an accidental situation from a nuclear facility is an important task to take into consideration in radiological safety assessment in order to obtain an approximation of the radiation effects on human health and safety.¹⁻⁵ Thus, once the radionuclide materials content released into the atmosphere is determined, it is necessary to perform a realistic assessment of radiological risk in order to characterize the radiation doses under accidental severe core damage conditions. In the case of a hypothetical accident in a research reactor, only a fraction of the entire inventory of radionuclides contained in the fuel must be released into the environment through the ventilation system. The release magnitude of radionuclides in the containment can be influenced by several factors, such as the amount and composition of radioactivity contained in the reactor core.

This work is a contribution to the evaluation of radiation doses of a hypothetical accident of 1 MW Triga Mark II re-

search reactor using HotSpot Health Physics Code (Fig. 1), developed at Lawrence Livermore National Laboratory, University of California, USA.^{6,7} The total damage of fuel element cladding with a maximum release of radioactivity from the reactor core and building was considered.⁵ The Hotspot code includes radiation dosimetry methodologies recommended by the International Commission on Radiological Protection (ICRP) and summarized in Federal Guidance Reports No. 11, 12, and 13.⁸⁻¹⁰ The FGR-13 methodology was adopted in the calculations using the new ICRP-66 lung model and ICRP series 60/70 methodologies.¹¹

For this purpose, the time-integrated air concentration, the ground deposition, and the total effective dose (TED) assessment on the environment and the public at various downwind distance were calculated for short-time releases. The TED represents the radioactive material producing the equivalent dose, which summarizes all combined doses that could be external or internal to the body from all applicable delivery pathways (inhalation, immersion,

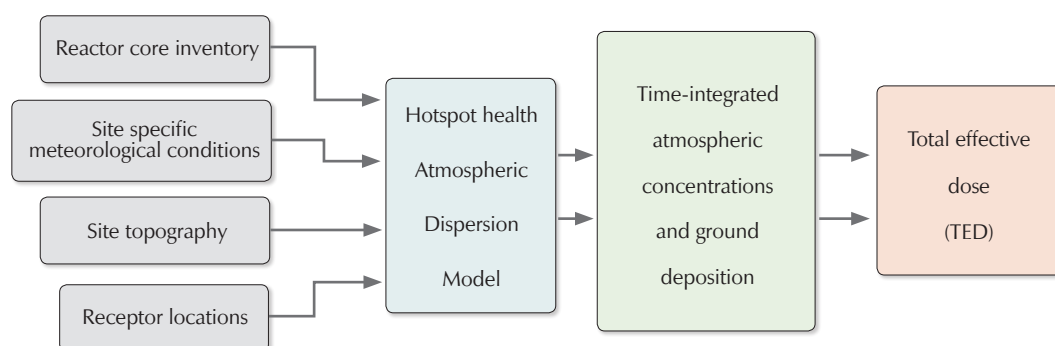


Fig. 1 – General Methodology calculation by HotSpot code^{6,7}

* Corresponding author: Ahmed Dahia, PhD
Email: dahia.univ@gmail.com

resuspension, and ground shine) resulting from the release of radionuclides during the accident.¹² The external exposure is determined by the radiation emitted by the radionuclides and absorbed by the body, and the internal exposure is the result of the incorporation of deposit material into the human body by inhalation or ingestion.¹³ The postulated accident scenario is similar to that described by Villa et al.⁵

The selected possible hazardous radionuclides which define the source term have been exploited as an input for air dispersion modelling and radiation dose calculations using meteorological data of the site. Only noble gases and halogens were considered in this study since they are viewed as volatile nuclides, and will decay and deposit their energy into the ecosystem, thus contributing to radiation risk and threat to human health.

2 Materials and methods

2.1 Site-specific meteorological conditions

The HotSpot Health Physics Code was used for the assessment of TED in emergency conditions. The diffusion characteristics were assumed to remain constant throughout the release, and two deposition velocities were considered; 0.3 cm s⁻¹ for respirable particles, and 8 cm s⁻¹ for non-respirable particles. A value of 320 m for the inversion layer height was chosen. The meteorological observations at the site indicated that west-northwest (WNW) was the dominant direction of wind with 1 m s⁻¹ wind speed.⁵ The TED calculation was evaluated at 5 km distance from the source.

2.2 Stability classes

Plume diffusion in HotSpot code is based on Pasquill-Gifford (PG) stability widely used in Gaussian plume dispersion models as illustrated in Table 1.¹⁴ The stability classes are generally defined using letter designations from A to F, where A represents the most unstable atmospheric conditions, B unstable, C slightly unstable, D neutral, E slightly stable, and F represents the most stable. In addition, for extremely stable conditions an additional stability class G

Table 1 – Summary of test conditions¹⁴

Wind speed/ m s ⁻¹	Day time insolation			Night time	
	Strong	Moderate	Slight	Thin overcast >4/8 low cloud cover	<cloud cover
<2	A			A–B	
2–3	A–B			B	
3–5	B			B–C	
5–6	C			C–D	
>6	C			C	

is defined.¹⁵ In this work, it was assumed that the relevant stability class E (slightly stable) was predominant justifying its use in this study. However, other stability classes of A~C were taken for comparison purposes.

2.3 Dispersion modelling

The Gaussian numerical approach of continuous release was used in HotSpot to determine the atmospheric concentration of aerosol. The Gaussian Eq. (1), described as follows, includes all the necessary data for dispersion calculation: atmospheric conditions (speed and direction of the wind), different atmospheric stabilities, flow rate, coefficient diffusion, and effective release height.

$$C(x, y, z, H) = \frac{Q}{2\pi u \sigma_y \sigma_z} \exp\left(-\frac{y^2}{2\sigma_y^2}\right) \left\{ \exp\left[-\frac{(z-H)^2}{2\sigma_z^2}\right] + \exp\left[-\frac{(z+H)^2}{2\sigma_z^2}\right] \right\} \exp\left(-\frac{\lambda x}{u}\right) \quad (1)$$

If the mixing layer height (L) is considered, and the vertical standard deviation exceeds the inversion height, Eq. (1) becomes:

$$C(x, y, z, H) = \frac{Q}{\sqrt{2\pi} u \sigma_y L} \exp\left(-\frac{y^2}{2\sigma_y^2}\right) \exp\left(-\frac{\lambda x}{u}\right) \quad (2)$$

where $C(x, y, z, H)$ is the time-integrated atmospheric concentration ((Bq s m⁻³) for a source term Q (Bq). H is the effective release height (m), u is the average wind speed at the effective release height (m s⁻¹), σ_y and σ_z are the standard deviations of the concentration distribution in lateral and vertical directions (m), respectively,^{14,16} λ is the radioactive decay constant (s⁻¹), x is the downwind distance from the source (m), y and z are the crosswind and vertical axis distance (m), respectively, where the coordinates x , y , z are oriented in the direction of the mean wind velocity. L describes inversion layer height (m).

2.3.1 Wind speed variation with height

To adjust the wind speed for all effective release heights, HotSpot uses the following relationship, Eq. (3), between the effective release height H and altitude z , which is frequently measured at a normative high of 10 m.

$$u(H) = u(z) \left(\frac{H}{z}\right)^p \quad (3)$$

where $u(z)$ is wind speed at reference height (m s⁻¹), z is elevation (m), and p is exponential factor used for calculating wind speed variation with height estimated by Irwin.¹⁷ The values of 0.35 and 0.40 at standard and city terrain, respectively, for stability class E were considered.

2.3.2 TED calculation

The total effective dose (TED) is the most complete expression of the combined dose from all applicable delivery pathways. The TED is the sum of the committed effective dose equivalent (CEDE) from inhalation, defined by expression 4, and the effective dose equivalent (EDE) from external exposure such as submersion, ground shine, and resuspension. The TED should consider all radionuclides, and should be determined for the most limiting receptor at the outer boundary of different population zones using FGR-13 Dose Conversion Data.¹⁹ The CEDE reflects the dose equivalent received by a tissue or organ (lungs, liver, thyroid, etc.) of a target individual over a specific time interval T (s)⁷ during the release of radioactive material. The CEDE depends on the time-integrated atmospheric concentration C ($\text{Ci s}^{-1} \text{m}^{-3}$) and the dose conversion factor (DCF) ($\text{Sv m}^3 \text{Bq}^{-1} \text{s}^{-1}$).

$$\text{CEDE}(T) = C \times \text{DCF}(T) \tag{4}$$

2.3.3 Plume rise due to buoyancy calculation

HotSpot calculates both the momentum and the buoyant plume rise, and makes a comparison between the two greater results. The buoyancy flux F was defined by the following expression:¹⁸

$$F = r^2 g v \left(1 - \frac{T_a}{T_s} \right) \tag{5}$$

where v is stack exit velocity (m s^{-1}), r is stack radius (m), T_a and T_s are ambient air temperature and stack effluent temperature, respectively (K), g is gravitational acceleration ($= 9.8 \text{ m s}^{-2}$). The following Eq. (6) was introduced in HotSpot code to determine the effective release height due to plume rise:

$$H = h + \frac{1.6(F)^{1/3} (X^*)^{2/3}}{u(H)} \tag{6}$$

where H is effective release height (m), h is physical stack height (m), $u(H)$ is wind speed at effective release height (m s^{-1}), X^* is the distance associated to final effective release height (m), with:

$$X^* = 119F^{0.40} \quad \text{for } F \geq 55 \quad \text{and} \quad X^* = 49F^{0.625} \quad \text{for } F < 55 \tag{7}$$

2.4 Source term and accidental release scenario

The TED expected to be released into the environment was calculated as a function of downwind distance. The volatile radionuclides with a high risk of radiation for human health and radiological consequence gravity were analysed. The core inventory for each radionuclide, mainly noble gases and iodine fissions products, used as input for the atmospheric dispersion and dose assessment is shown

in Table 2.⁵ This mixture was based on physical and chemical properties of nuclides, their volatility and their contribution to collective dose, principally in the thyroid gland.⁶ The default value of receptor height was taken equal to 1.5 m.

In addition, it was assumed that only one fuel element's cladding was damaged, where only a fraction of the entire inventory was released under worst-case atmospheric conditions.⁵ The supposed release occurs at a height of 20 m, which coincides with the building height, and a wind speed of 1 m s^{-1} . In addition, the release fractions of the gaseous fission products with a higher degree of mobility, such as noble gases and halogens were considered. The release fractions of the radionuclide into the atmosphere applied to the calculated TED were taken from US-NRC regulatory guide⁴ 1.183, having values of 1, 0.4, 0.3, 0.05, and 0.02 for noble gases, halogens, alkali metals, the tellurium group and the Ba–Sr group, respectively.^{3,21} Weathering correction factors for nuclear fallout and deposition of radionuclides used in the present work are defined in the WASH 1400 (NUREG-75/014).^{20,21}

In the present work, the doses were calculated taking into account the following assumptions:

- Reactor is operated at 1 MW (t) power,
- Duration of release: 1-day and 50 years after shutdown,
- Considered radionuclides: noble gases and halogens.

Table 2 – Radionuclide inventory in the core, release fraction, and isotopic activity released into the atmosphere²

Nuclide	Core inventory /Bq	Group	Release fraction	Activity released /Bq
Kr-83m	$5.91 \cdot 10^{10}$	Noble gas	1	$5.91 \cdot 10^{10}$
Kr-85m	$1.39 \cdot 10^{11}$	Noble gas	1	$1.39 \cdot 10^{11}$
Kr-85	$2.22 \cdot 10^{10}$	Noble gas	1	$2.22 \cdot 10^{10}$
Kr-87	$2.81 \cdot 10^{11}$	Noble gas	1	$2.81 \cdot 10^{11}$
Kr-88	$3.97 \cdot 10^{11}$	Noble gas	1	$3.97 \cdot 10^{11}$
Xe-131m	$3.56 \cdot 10^9$	Noble gas	1	$3.56 \cdot 10^9$
Xe-133m	$2.18 \cdot 10^{10}$	Noble gas	1	$2.18 \cdot 10^{10}$
Xe-133	$7.45 \cdot 10^{11}$	Noble gas	1	$7.45 \cdot 10^{11}$
Xe-135m	$1.26 \cdot 10^{11}$	Noble gas	1	$1.26 \cdot 10^{11}$
Xe-135	$7.03 \cdot 10^{11}$	Noble gas	1	$7.03 \cdot 10^{11}$
Xe-138	$6.87 \cdot 10^{11}$	Noble gas	1	$6.87 \cdot 10^{11}$
I-129	$7.47 \cdot 10^4$	Halogen	0.4	$2.98 \cdot 10^4$
I-130	$7.16 \cdot 10^8$	Halogen	0.4	$2.86 \cdot 10^8$
I-131	$3.21 \cdot 10^{11}$	Halogen	0.4	$1.28 \cdot 10^{11}$
I-132	$4.77 \cdot 10^{11}$	Halogen	0.4	$1.90 \cdot 10^{11}$
I-133	$7.44 \cdot 10^{11}$	Halogen	0.4	$2.97 \cdot 10^{11}$
I-134	$8.40 \cdot 10^{11}$	Halogen	0.4	$3.36 \cdot 10^{11}$
I-135	$6.93 \cdot 10^{11}$	Halogen	0.4	$2.77 \cdot 10^{11}$

3 Results and discussion

3.1 Doses calculation

The mixture of volatile radionuclides is partially emitted into the atmosphere at an effective height of 20 m from the ground. Figs. 2 and 3 graphically illustrate the doses and ground deposition for 1-day and 50 years of exposure for stability class E (slightly stable) after shutdown of reactor. The TED results indicated that the dose values increased with distance, reached a maximum, and then decreased gradually with distance. The doses were minimal at the beginning of release after 1-day duration release, which yielded a maximum of $2.2 \cdot 10^{-12}$ Sv very close to the release point (within 0.1 km) (Fig. 2), with almost no radiation effects. For the same type of reactor, the results showed very good agreement with previous results obtained by Villa et al.,⁵ using the program system PC Cosyma. The TED reaches a maximum effective value of $5.90 \cdot 10^{-4}$ Sv at 480 m downwind distance from the source at an arrival time of less than six minutes (Fig. 2). Therefore, at 5 km from the release point, the TED is only $2.2 \cdot 10^{-3}$ mSv at an arrival time of 01 h:05 min. After 50 years' duration release and

at the same distance, the maximum effective dose reaches a value of $3.5 \cdot 10^{-5}$ Sv (Fig. 2). This increase in the dose is due to the effect of wind, which favours the diffusion factor in cross and vertical directions. Hence, the plume centre-lines ground deposition is shown in Fig. 3, which revealed a similar trend in both scenarios. Noble gases are inert and will not contribute to ground deposition.

Consequently, we may conclude that these values are satisfactory, since they are considerably below the annual dose regulatory limits of 1 mSv for the public, as set by IAEA Safety Standards for protecting people and the environment.^{18,23} Therefore, this situation constitutes no health risk for individuals affected by these low levels of exposure during the plume passage, and no emergency interventions or countermeasures, such as evacuation and supply of iodine tablets are required.

The TED calculation was also performed for comparison of other atmospheric stability classes (A~G) with wind speed of 1 m s^{-1} . As shown in Fig. 4, the more unstable meteorological conditions at the site give higher values at a shorter distance (1 h). The maximum calculated TED of

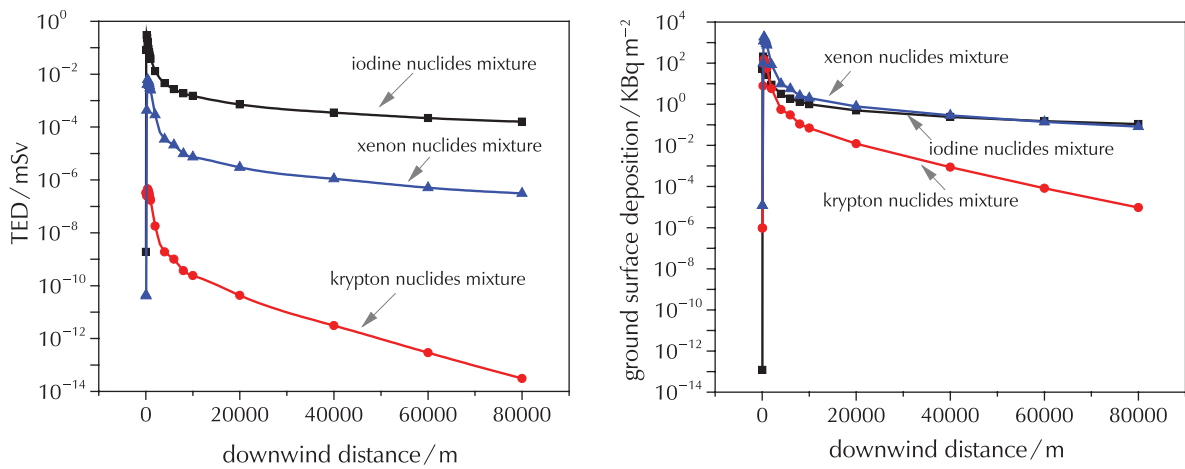


Fig. 2 – Evolution of plume centreline TED and ground deposition as function of downwind distance after 1-day after release

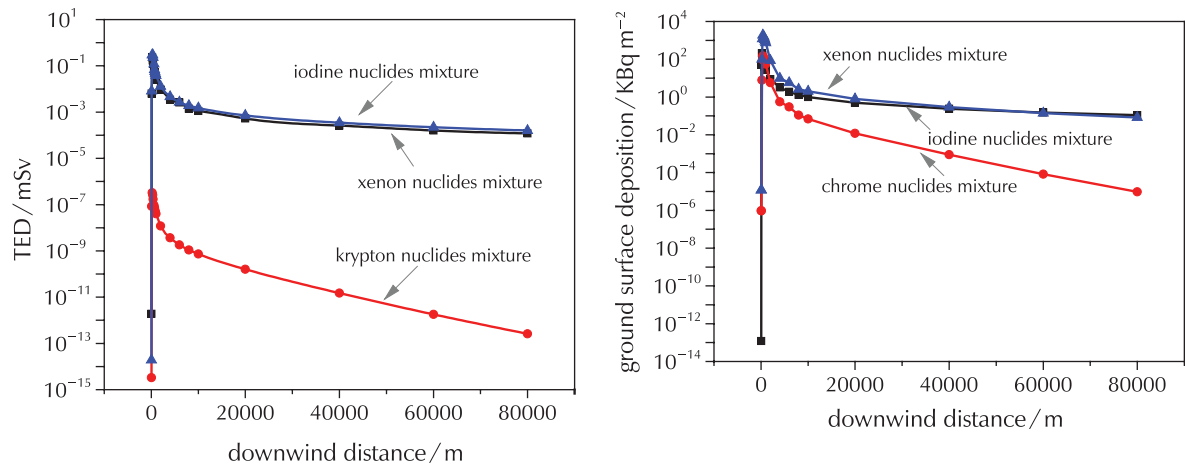


Fig. 3 – Evolution of plume centreline TED and ground deposition as function of downwind distance after 50 years after release

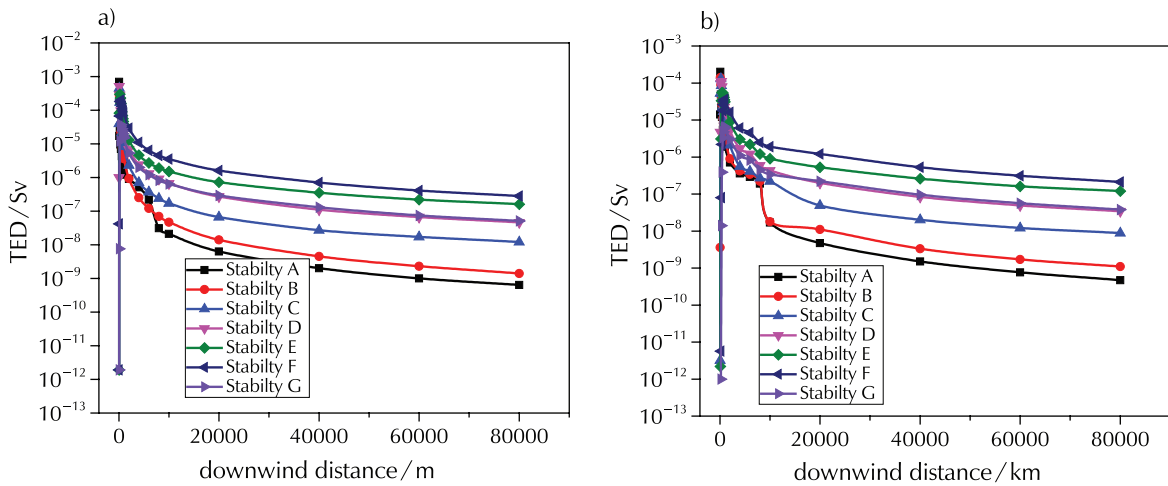


Fig. 4 – Evolution of plume centreline TED of mixture as function of downwind distance after (a) 1-day, and (b) 50 years' duration releases for different stability classes

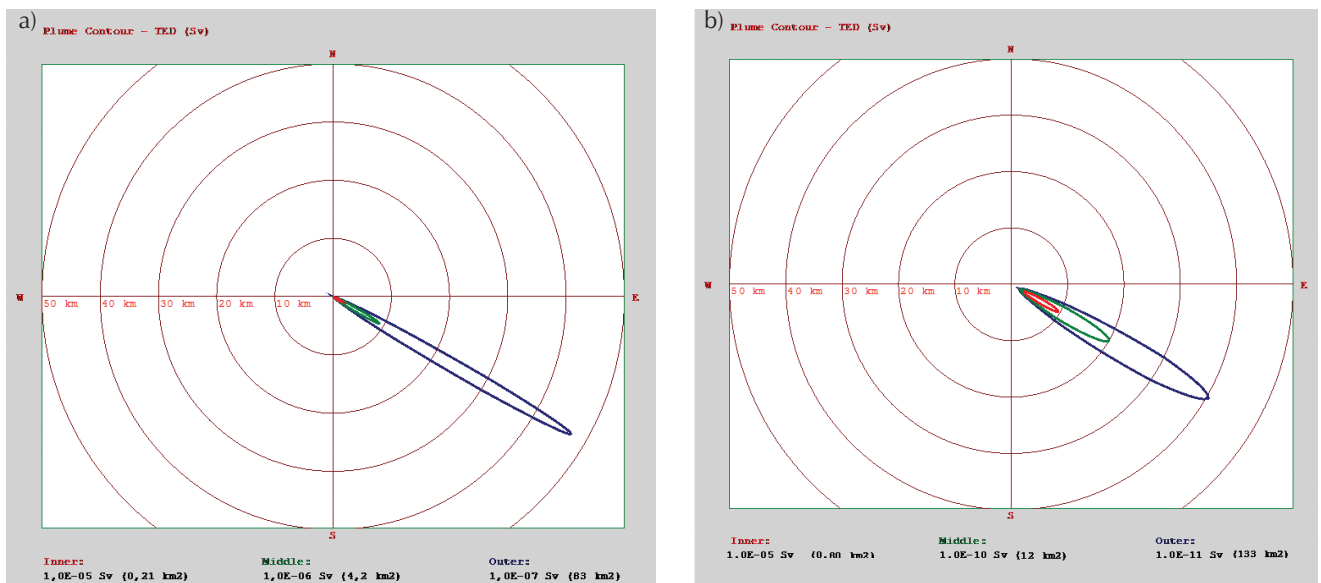


Fig. 5 – Plume contour lines of mixture as function a downwind distance to receptor location for (a) 1-day, and (b) 50 years after release

$1.84 \cdot 10^{-4}$ Sv is reached at 68 m for the stability class “A (very unstable)”, which is lower than the personnel annual effective dose limits. The model typically assumes maximum fluctuations in wind direction for stability class “A”. This results in greater plumes and great diffusion of concentrations. The same conclusions were found for the same type of reactor operated elsewhere by Hawley and Kathren.^{2,5,24-26} For the more stable atmospheric conditions, the maximum TED value decreases to a lower value due to less plume depletion (Fig. 4).

In addition, the TED plume contour for slightly stable class E with wind velocity of 1 m s^{-1} and for 1-day and 50 years after release is shown in Fig. 5, with three marked contours; red, green, and blue for $1.0 \cdot 10^{-5}$, $1.0 \cdot 10^{-6}$ and $1.0 \cdot 10^{-7}$ Sv, respectively. The red colour characterizes the higher dose risk for the population. These distinct regions

correspond to three boundary contour line areas of 0.21, 4.2, and 63 km^2 for 1-day duration release. Moreover, Fig. 5(b) shows three regions of the same TED contour line for 50 years duration release with 0.6, 12, and 133 km^2 , respectively. According to these results, we can conclude that the calculated TED in and around the area are significantly lower than the dose limits for personnel and population described in the international regulatory guides.^{18,22,23,27}

Moreover, multiple pathways from atmospheric transport releases are identified, including; internal exposure due to inhalation from resuspension of the airborne nuclides removed from the contaminated air, and external radiation exposure due to radionuclides in the plume and deposited on the ground. The dose results are shown in Figs. 6(a) and (b). From the results, it is obvious that the submersion and inhalation doses are more significant and dominant for

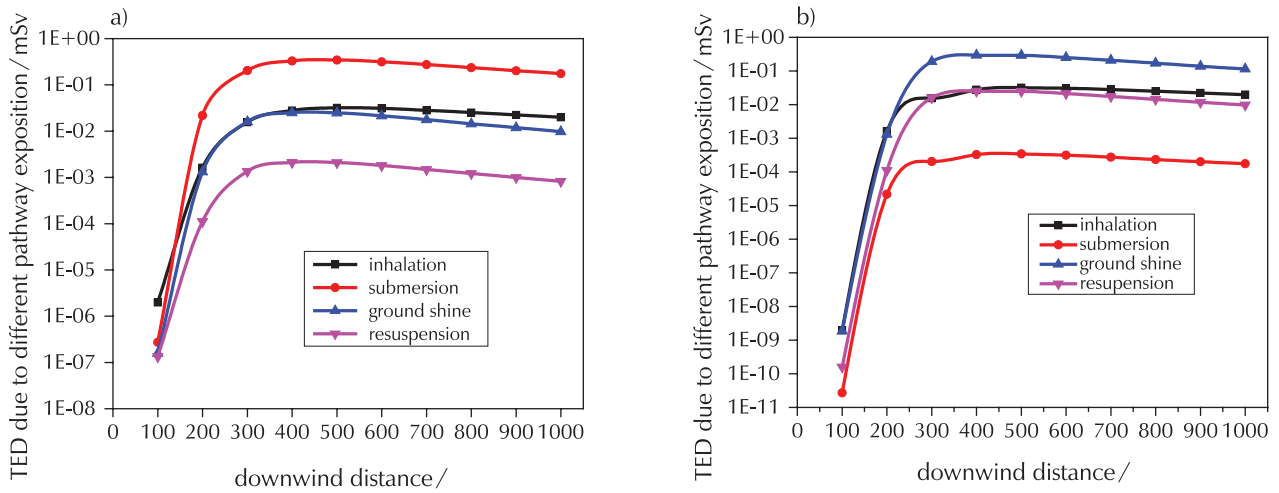


Fig. 6 – TED due to multiple pathways exposure in different downwind distance for a) 1-day, and b) 50 years' duration release

the TED compared to the other exposure pathway, such as ground shine and resuspension at 1-day duration release, while the ground shine is a more dominant pathway at 50 years' duration release after 300 m downwind distance. Different doses are very low close to the source, increasing quickly then decreasing slightly with time and distance. For this, it is recommended to take precautionary measures to protect members of the public against the exposure arising from these pathways in case of accidents away from the source.²⁸

3.2 Organ committed effective dose equivalent results and analysis

The committed dose equivalent (CEDE) includes dose equivalents for internal body organ or tissues, which have absorbed radiation after the intake of radioactive material.¹² Tables 3 and 4, and Fig. 7 give an overview of the CEDE distribution in the human body as a function of downwind distance after a one-day release and a 50 years after release. Three organs more sensitive to radiation were chosen in this study;¹² the thyroid gland, the lung, and skin. The human body dose was obtained by ingestion or inha-

Table 3 – CEDE for representative human body organ as a function of downwind distance at different arrival time intervals for 1-day after release

Distance /km	Organ dose /mSv			Arrival time /hr:min
	Thyroid	Lung	Skin	
0.1	$3.4 \cdot 10^{-9}$	$1.9 \cdot 10^{-9}$	$4.4 \cdot 10^{-8}$	00:01
0.2	$2.8 \cdot 10^{-2}$	$1.5 \cdot 10^{-2}$	$7.4 \cdot 10^{-2}$	00:02
0.3	$3.4 \cdot 10^{-1}$	$1.9 \cdot 10^{-1}$	$8.2 \cdot 10^{-1}$	00:03
0.4	$5.2 \cdot 10^{-1}$	$2.9 \cdot 10^{-1}$	$1.4 \cdot 10^0$	00:05
0.5	$5.2 \cdot 10^{-1}$	$2.9 \cdot 10^{-1}$	$1.4 \cdot 10^0$	00:06
0.6	$4.5 \cdot 10^{-1}$	$2.5 \cdot 10^{-1}$	$1.3 \cdot 10^0$	00:07
0.7	$3.7 \cdot 10^{-1}$	$2.1 \cdot 10^{-1}$	$1.1 \cdot 10^0$	00:09
0.8	$3.0 \cdot 10^{-1}$	$1.7 \cdot 10^{-1}$	$9.6 \cdot 10^{-1}$	00:10
0.9	$2.5 \cdot 10^{-1}$	$1.4 \cdot 10^{-1}$	$8.2 \cdot 10^{-1}$	00:11
1	$2.0 \cdot 10^{-1}$	$1.1 \cdot 10^{-1}$	$7.1 \cdot 10^{-1}$	00:13
2	$2.3 \cdot 10^{-2}$	$1.3 \cdot 10^{-2}$	$1.9 \cdot 10^{-1}$	00:26
4	$2.7 \cdot 10^{-3}$	$1.5 \cdot 10^{-3}$	$6.0 \cdot 10^{-2}$	00:52
5	$1.6 \cdot 10^{-3}$	$8.9 \cdot 10^{-4}$	$4.3 \cdot 10^{-2}$	01:05
8	$7.3 \cdot 10^{-4}$	$4.1 \cdot 10^{-4}$	$2.4 \cdot 10^{-2}$	01:44
10	$5.5 \cdot 10^{-4}$	$3.1 \cdot 10^{-4}$	$1.8 \cdot 10^{-2}$	02:10

Table 4 – CEDE for representative human body organ as a function of downwind distance at different arrival time intervals for 50 years' duration release

Distance /km	Organ dose /mSv			Arrival time /hr:min
	Thyroid	Lung	Skin	
0.1	$3.3 \cdot 10^{-10}$	$2.0 \cdot 10^{-10}$	$4.0 \cdot 10^{-8}$	00:01
0.2	$2.4 \cdot 10^{-3}$	$1.3 \cdot 10^{-3}$	$3.6 \cdot 10^{-2}$	00:02
0.3	$2.9 \cdot 10^{-2}$	$1.6 \cdot 10^{-2}$	$3.5 \cdot 10^{-1}$	00:03
0.4	$4.5 \cdot 10^{-2}$	$2.5 \cdot 10^{-2}$	$6.2 \cdot 10^{-1}$	00:05
0.5	$4.4 \cdot 10^{-2}$	$2.5 \cdot 10^{-2}$	$7.0 \cdot 10^{-1}$	00:06
0.6	$3.8 \cdot 10^{-2}$	$2.2 \cdot 10^{-2}$	$6.7 \cdot 10^{-1}$	00:07
0.7	$3.2 \cdot 10^{-2}$	$1.8 \cdot 10^{-2}$	$6.1 \cdot 10^{-1}$	00:09
0.8	$2.6 \cdot 10^{-2}$	$1.5 \cdot 10^{-2}$	$5.4 \cdot 10^{-1}$	00:10
0.9	$2.1 \cdot 10^{-2}$	$1.2 \cdot 10^{-2}$	$4.8 \cdot 10^{-1}$	00:11
1	$1.8 \cdot 10^{-2}$	$9.9 \cdot 10^{-3}$	$4.2 \cdot 10^{-1}$	00:13
2	$2.1 \cdot 10^{-3}$	$1.2 \cdot 10^{-3}$	$1.5 \cdot 10^{-1}$	00:26
4	$2.6 \cdot 10^{-4}$	$1.6 \cdot 10^{-4}$	$5.6 \cdot 10^{-2}$	00:52
5	$1.6 \cdot 10^{-4}$	$1.0 \cdot 10^{-4}$	$4.1 \cdot 10^{-2}$	01:05
8	$7.5 \cdot 10^{-5}$	$4.9 \cdot 10^{-5}$	$2.3 \cdot 10^{-2}$	01:44
10	$5.7 \cdot 10^{-5}$	$3.7 \cdot 10^{-5}$	$1.7 \cdot 10^{-2}$	02:10

lation process, which takes into account the metabolism of radioisotopes in the body, type and level of energy of the emitted radiations, and radio-sensitivity of the organs.²⁹ It was observed that the calculated CEDE are lower, and the highest value primarily affects the thyroid followed by the skin, and thirdly the lungs.¹² The maximum value for this organ is about $7.0 \cdot 10^{-1}$ mSv occurring at a distance of 0.5 km from the source with arrival time of six minute, and it is about $4.1 \cdot 10^{-2}$ mSv at 5 km from the source with arrival time of 01 h : 05 min.

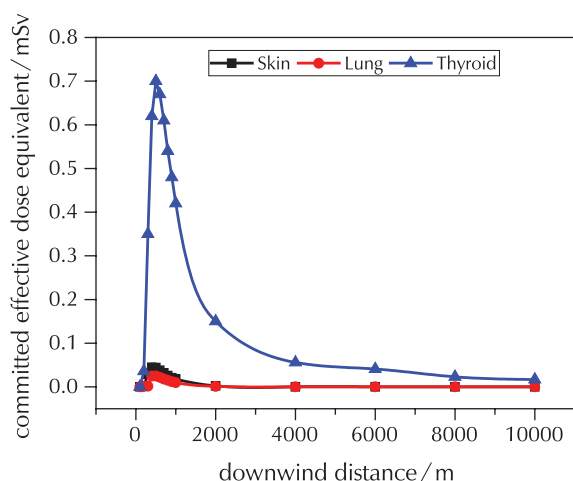


Fig. 7 – CEDE profile as function of downwind distance

3.3 Air concentration calculation

The results of time-integrated air concentration around the affected site show a difference in the concentrations in different time releases (Fig. 8). The figure shows that the calculated concentration increase reached a maximum then decreased for the 1-day after release. The maximum value reached was approximately $1.0 \cdot 10^4$ kBq s m⁻³ at 500 m downwind distance, corresponding to the TED of $5.9 \cdot 10^{-2}$ mSv. The air concentration for the second scenario of 50 years' release duration was much smaller. The highest value reached was less than $1.0 \cdot 10^2$ Bq s m⁻³ at the same conditions. This loss of concentration over the years was due to the radioactive decay under the effect of leaching, the meteorological conditions and the half-life of the released radioisotopes. Analysing the results reveals also that the cumulative concentrations near the reactor site have a strong impact on the transported cloud in various wind directions, and consequently, on the total dose received by population surrounding nuclear site from different pathways of exposure.³⁰

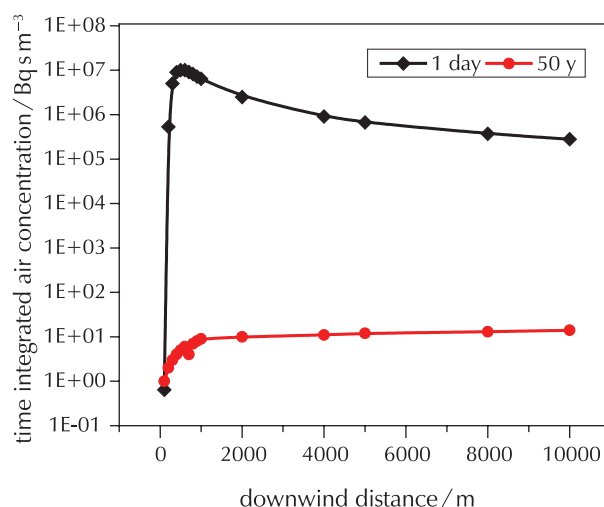


Fig. 8 – Time-integrated air concentration as function of downwind distance to receptor location for both durations of release

3.4 Ground shine dose rate calculation for various pathways

The ground shine is defined as the radiation produced by radioactive materials on the surface. Depending on the type and amount of radiation being produced, this may or may not have significant health consequences.⁷ For a realistic prediction of the concentration of deposit material on the ground, it is important to know the values of ground shine dose rate. For this, the ground-shine dose rates of iodine, xenon, and radionuclide mixture for a receptor location were calculated, and are presented in Fig. 9. The results indicate that the dose rate is more important in 1-day after release for all cases of mixture.

4 Conclusion

Radiological safety assessment of a selected site was analysed for comparison purposes in order to predict the radiological consequences. The TED and ground deposition were considered after 1 day and 50 years' duration release. It was found that the TED values increased severely and reached a peak of $5.9 \cdot 10^{-4}$ Sv at 480 m from the source at an arrival time of about six minutes, and reached a maximum of $3.5 \cdot 10^{-5}$ Sv at the same distance after 50 years of release. These values are below the annual regulatory limits of 1 mSv for the public. In addition, it may be concluded that there is no increase in the potential radiological impact on public health. Consequently, the inhalation doses resulting from the accident were not very significant, and were higher compared with the rest exposure pathways.

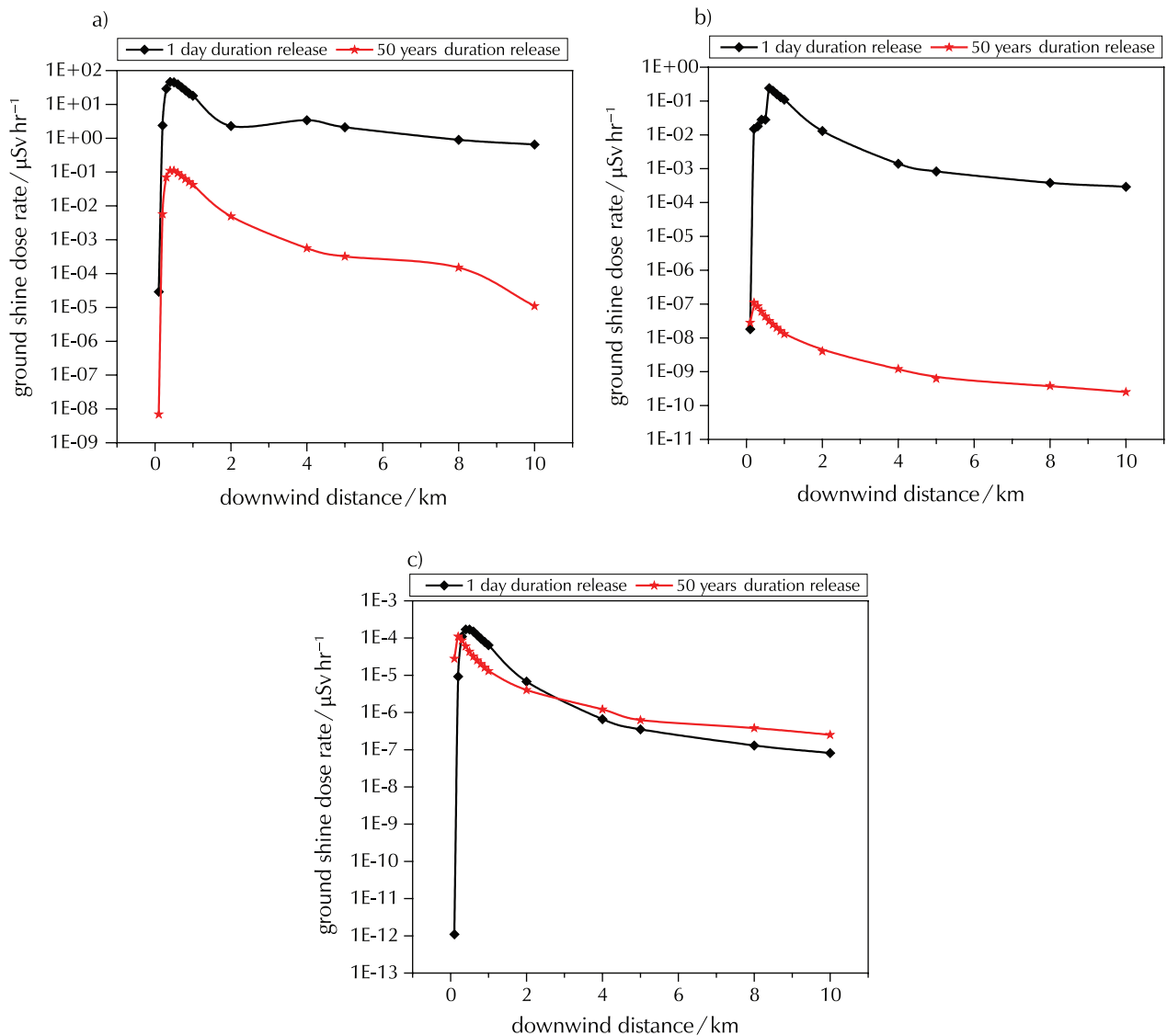


Fig. 9 – Ground shine dose rate evolution of mixture as a function of downwind distance to receptor location for both time durations of release: a) Iodine nuclides mixture, b) Xenon nuclides mixture, c) Krypton nuclides mixture

The comparative study also indicated that the calculation tool chosen can offer screening capabilities, and some practical approximation for a response action can be derived for an emergency planning situation for a hypothetical accident of 1 MW research reactor TRIGA Mark-II.

ACKNOWLEDGEMENTS

This work was supported by the Algerian Atomic Energy Commission (COMENA). The authors thank the Nuclear Research Centre of Birine for their the help with this work.

List of abbreviations and symbols

TED	– total effective dose
CEDE	– committed effective dose equivalent
EDE	– effective dose equivalent from external exposure
$C(x,y,z,H)$	– time-integrated air concentration
DCF	– dose conversion factors
H	– effective release height
h	– physical stack height
$u(H)$	– wind speed at effective release height
X^*	– distance associated to the final effective release height
Q	– source term
σ_y and σ_z	– standard deviations in lateral and vertical directions
λ	– radioactive decay constant
L	– inversion layer height

References

Literatura

1. J. L. Muswema, E. O. Darko, J. Gbadago, E. K. Bofo, Atmospheric dispersion modeling and radiological safety analysis for a hypothetical accident of Ghana Research Reactor-1 (GHARR-1), *Ann. Nucl. Energy* **68** (2014) 239–246, doi: <https://doi.org/10.1016/j.anucene.2014.01.029>.
2. J. L. Muswema, B. G. Ekoko, V. M. Lukanda, J. K. K. Lobo, E. O. Darko and E. K. Bofo, Source term derivation and radiological safety analysis for the TRICO II research reactor in Kinshasa, *Nucl. Eng. Des.* **281** (2015) 51–57, doi: <https://doi.org/10.1016/j.nucengdes.2014.11.014>.
3. R. S. Shoaib, M. Iqbal, Atmospheric dispersion modeling for an accidental release from the Pakistan research reactor-1 (PARR-1), *Ann. Nucl. Energy* **32** (2005) 1157–1166, doi: <https://doi.org/10.1016/j.anucene.2005.03.008>.
4. Y. Zhu, J. Guo, C. Nie, and Y. Zhou, Simulation and dose analysis of a hypothetical accident in Sanmen Nuclear Power Plant, *Ann. Nucl. Energy* **65** (2014) 207–213, doi: <https://doi.org/10.1016/j.anucene.2013.11.016>.
5. M. Villa, M. Haydn, G. Steinhauer, H. Bock, Accident scenarios of the TRIGA Mark II reactor in Vienna, *Nucl. Eng. Des.* **240** (2010) 4091–4095, doi: <https://doi.org/10.1016/j.nucengdes.2010.10.001>.
6. S. A. Birikorang, R. G. Abrefah, Radiological dose assessment for Ghana Research Reactor-1 at shutdown using dispersion model: Conversion from high-enriched Uranium to Low-Enriched Uranium Fuel, *J. Env. Res. Eng. Man.* **74** (2018) 21–35, doi: <https://doi.org/10.5755/j01.arem.74.1.19948>.
7. S. G. Homann, F. Aluzzi, HotSpot Health Physics Codes Version 3.1.2 User's Guide, LLNL-SM- 636474, National Atmospheric Release Advisory Center, (2020), Lawrence Livermore National Laboratory, Livermore, CA, USA.
8. K. F. Eckerman, A. B. Wolbarst, A. C. B. Richardson, Limiting values of radionuclide intake in air concentration and dose conversion factors for inhalation submersion, and ingestion, Federal Guidance Report No. 11, USA, 1998, doi: <https://doi.org/10.2172/6294233>.
9. K. F. Eckerman, J. C. Ryman, External exposure to radionuclides in air, water and soil, Federal Guidance Report No. 12, 1993, Washington DC, USA.
10. K. G. Veinot, K. F. Eckerman, M. B. Bellamy, M. M. Hiller, S. A. Dewji, C. E. Easterly, N. E. Hertel, R. Manger, Effective dose rate coefficients for exposure to contaminated soil, *Rad. Environ. Phys.* **56** (2017) 255–267, doi: <https://doi.org/10.1007/s00411-017-0692-7>.
11. S. G. Homann, HotSpot Health Physics Codes Version 2.07.1 User's Guide, National Atmospheric Release Advisory Center, Lawrence Livermore National Laboratory, Livermore, CA 94550, (2010), LLNL-TM-411345 Rev. 1, Calif, USA.
12. C. Bo, Z. Junxiao, C. Yixue, Radiation dose calculations for a hypothetical Accident in Xianning Nuclear Power Plant, *Sci. Technol. Nucl. Install.* **2016** (2016) 3105878, doi: <https://doi.org/10.1155/2016/3105878>.
13. A. F. M Rahman, M. Shamsuzzaman, M. S. Rahman, K. Uddin, S. Yeasmin, H. M. Nazmul Haque, M. M. Akramuzzaman, R. C. Shyamal, Assessment of radiological dose around a 3-MW TRIGA Mark-II Research Reactor, *Int. Lett. Chem. Phys. Astron.* **15** (2013) 183–200, doi: <https://doi.org/10.18052/www.Scipress.com/ILCPA.15.183>.
14. F. Pasquill, Atmospheric dispersion of pollution, *Q. J. R. Meteorol. Soc.* **97** (1971) 369–395, doi: <https://doi.org/10.1002/qj.49709741402>.
15. D. B. Turner, Workbook of atmospheric dispersion estimates: an introduction to dispersion modeling, 2nd ed., Lewis Publishers, Boca Raton, 1994.
16. S. M. E. Khaled, M. Fawzia, A. K. Sanaa, Comparison of some sigma schemes for estimation of air pollutant dispersion in moderate and low winds, *Atmos. Sci. Lett.* **6** (2005) 90–96, doi: <https://doi.org/10.1002/asl.94>.
17. J. S. Irwin, A theoretical variation of the wind profile power law exponent as a function of surface roughness and stability, *Atmos. Environ.* **13** (1979) 191–194, doi: [https://doi.org/10.1016/0004-6981\(79\)90260-9](https://doi.org/10.1016/0004-6981(79)90260-9).
18. ICRP, International Commission on Radiological Protection, Human respiratory tract model for radiological protection, ICRP 66, *Annals of ICRP* **24** (1994) 1–3, url: <https://www.icrp.org/publication.asp?id=icrp%20publication%2066>.
19. C. A. Margeanu, Comparative Study on Radiological Impact due to Direct Exposure to a Radiological Dispersal Device using a Sealed Radiation Source, in Tenth Radiation Physics & Protection Conference, Nasr City – Cairo, Egypt, 2010, pp. 311–320, url: https://inis.iaea.org/collection/NCLCollectionStore/_Public/42/076/42076656.pdf.
20. IAEA, International Atomic Energy Agency, Reactor safety study, An assessment of accident risks in U.S commercial Nuclear Power Plant (1975), Wash-1400 (NUREG 75/014).
21. ICRP, US-NRC, Nuclear Regulatory Commission, Alternative radiological source terms for evaluating design basis accidents at Nuclear Power Reactors, (2000), Regulatory Guide 1.183.
22. IAEA, International Atomic Energy Agency, Radiation protection and safety of radiation sources: International Basic Safety Standards, General Safety Requirements Part 3 (2014), Vienna, Austria.
23. ICRP, International Commission on Radiological Protection, Age-dependent Doses to the Members of the Public from Intake of Radionuclides – Part 5 Compilation of Ingestion and Inhalation Coefficients. ICRP Publication 72, (1995), Ann. ICRP 26 (1).
24. S. C. Hawley, R. L. Kathren, Credible accident analyses for TRIGA and TRIGA-fueled reactors, Report. Pacific Northwest Laboratory, 1982, Richland, WA, USA.
25. A. Anvari, L. Safarzadeh, Assessment of the total effective dose for accidental release from the Tehran Research Reactor, *Ann. Nucl. Energy* **50** (2012) 251–255, doi: <https://doi.org/10.1016/j.anucene.2012.07.002>.
26. M. A. Malek, K. J. A. Chisty, M. M. Rahman, Dose distribution of ¹³¹I, ¹³²I, ¹³³I, ¹³⁴I, and ¹³⁵I due to a hypothetical accident of TRIGA Mark-II research reactor, *Int. J. Basic Appl. Sci.* **1** (2012) 244–259, doi: <https://doi.org/10.14419/ijbas.v1i3.110>.
27. ICRP, International Commission on Radiological Protection, 1990 Recommendations of the International Commission on Radiological Protection, ICRP 60, *Annals of ICRP*, **21**(1991) 1–3.
28. IAEA, International Atomic Energy Agency, Safety reports series N° 64. Programmes and systems for source and environmental radiation monitoring. Vienna, 2010.
29. J. L. Muswema, G. B. Ekoko, J. K. K. Lobo, V. M. Lukanda, TRICO II core inventory calculation and its radiological consequence analyses, *J. Nucl. Rad. Sci.* **2** (2) (2016) 024501, doi: <https://doi.org/10.1115/1.4031772>.
30. A. Dahia, Dj. Merrouche, T. Rezoug, Radioactive contamination control by atmospheric dispersion assessment of airborne indicator contaminants: numerical model validation, *Environ. Mod. Ass.* **23** (2018) 401–414, doi: <https://doi.org/10.1007/s10666-018-9598-2>.

SAŽETAK

Usporedna studija doze zračenja hipotetske nesreće u istraživačkom reaktoru

Ahmed Dahia, Djemai Merrouche, Amel Dadda i Amina Lyria Cheridi*

Ovo istraživanje doprinos je izračunima doze zračenja hipotetske nesreće istraživačkog reaktora Triga Mark II od 1 MW primjenom HotSpot koda. Razmatrano je slučajno oslobađanje plemenitih plinova i halogena. Određena je vrijednost ukupne učinkovite doze nakon 1 dana i nakon 50 godina. Razmatrano je ukupno oštećenje obloge dijela s maksimalnom radioaktivnošću. Dobi-
veni rezultati pokazuju minimalne vrijednosti ukupne učinkovite doze na početku ispuštanja i na manjoj udaljenosti od izvora. Maksimalni rezultati izračuna su prihvatljivi i ispod preporučenog doznog ograničenja.

Ključne riječi

Godišnja učinkovita doza, disperzija u atmosferi, ukupna učinkovita doza, CEDE, HotSpot kod, sigurnosna analiza

Nuclear Research Center of Birine, B.P 180 Ain Oussera, Djelfa, 17 200, Alžir

*Izvorni znanstveni rad
Prispjelo 5. prosinca 2021.
Prihvaćeno 17. siječnja 2022.*